Original Article

Identification of hub genes and key modules in laryngeal squamous cell carcinoma

Hongyue Li, Shaojun Bo, Yutian Guo, Tiantian Wang, Yangwang Pan

Department of Otolaryngology Head and Neck Surgery, Civil Aviation General Hospital (Peking University Civil Aviation School of Clinical Medicine), Beijing, China

Contributions: (I) Conception and design: H Li; (II) Administrative support: S Bo; (III) Provision of study materials or patients: None; (IV) Collection and assembly of data: Y Guo; (V) Data analysis and interpretation: T Wang, Y Pan; (VI) Manuscript writing: All authors; (VII) Final approval of manuscript: All authors.

Correspondence to: Hongyue Li, MM. Department of Otolaryngology Head and Neck Surgery, Civil Aviation General Hospital (Peking University Civil Aviation School of Clinical Medicine), No. 76 Chaoyang Road, Chaoyang District, Beijing 100123, China. Email: xjtuhongyueli@163.com.

Background: Laryngeal squamous cell carcinoma (LSCC) is the prominent cancer in head and neck, which greatly affects life quality of patients. The pathogenesis of LSCC is not clear. Presently, the LSCC treatments include chemotherapy, surgery and radiotherapy; however, these methods have poor efficacy in patients with recurrent and persistent cancer. Therefore, the study identified the hub genes accompanied with LSCC, which may be a potential therapeutic target in the future.

Methods: We extracted whole transcriptome high-throughput sequencing (HTS) LSCC data from The Cancer Genome Atlas (TCGA) and Gene Expression Omnibus (GEO) databases and calculate differentially expressed genes (DEGs) between LSCC and normal samples using statistical software RStudio. Through weighted gene co-expression network analysis (WGCNA), enrichment examination of Kyoto Encyclopedia of Genes and Genomes (KEGG) pathways and Gene Ontology (GO) functions, and examination of protein-protein interaction (PPI) network, we obtained network hub genes and validated the hub genes prognostic value and expression levels of protein.

Results: Through analysis of differential gene expression, from the GEO and TCGA databases 2,139 and 2,774 DEGs were obtained, respectively, 13 and 15 modules were screened from TCGA-LSCC and GSE127165 datasets by WGCNA, respectively. The most significant positive and negative correlation modules in the WGCNA and DEG lists were overlapped, and overall 36 co-expressed overlapping genes were retrieved. Through enrichment analysis of GO and KEGG, it was found that the gene functions were highly concentrated in cell junction assembly, basement membrane, extracellular matrix (ECM) structural constituent etc., and the pathways were mainly concentrated in ECM receptor interaction, focal adhesion, small cell lung cancer, and toxoplasmosis. Through analysis of PPI network analysis, 10 network hub genes (*SNAI2*, *ITGA6*, *LAMB3*, *LAMC2*, *CAV1*, *COL7A1*, *GJA1*, *EHF*, *OAT*, and *GPT*) were obtained. Finally, survival analysis and protein expression validation of these genes confirmed that low *OAT* expression and high *CAV1* expression remarkably influenced the survival of patient's prognosis with LSCC.

Conclusions: We recognized the hub genes and key modules nearly associated to LSCC and these genes were validated by survival analysis and the database of Human Protein Atlas (HPA), which is of high importance for unveiling the pathogenesis of LSCC and probing for new precise biological marker and potential therapeutic targets.

Keywords: Laryngeal squamous cell carcinoma (LSCC); key modules; hub genes; comprehensive bioinformatic analysis

Submitted Jan 14, 2024. Accepted for publication May 30, 2024. Published online Jul 16, 2024.
doi: 10.21037/tcr-24-104
View this article at: https://dx.doi.org/10.21037/tcr-24-104

Introduction

Laryngeal squamous cell carcinoma (LSCC) is the prominent cancer in head and neck, which greatly affects life quality of patients. According to the latest European Head and Neck Society (EHNS)-European Society for Medical Oncology (ESMO)-European Society for Radiotherapy and Oncology (ESTRO) clinical practice guidelines, the incidence is 4.6/100,000 and the year relative survival rate is 61% (1). The pathogenesis of LSCC is not clear and is presently believed in the involvement of the synergistic effect of numerous carcinogenic factors like alcohol consumption, smoking, human papillomavirus (HPV) infection and environmental factors (2). Presently, the LSCC treatments include chemotherapy, surgery and radiotherapy; however, these methods have poor efficacy in patients with recurrent and persistent cancer (3). Therefore, there is an urgent need to recognize the hub genes accompanied with LSCC and identify novel therapeutic targets.

With modern creation evolution of genomics and high-throughput sequencing (HTS) technology, numerous gene datasets store a high quantity disease gene expression information and clinical information (4,5), which lays a foundation for evaluating the mechanism of disease at the molecular level and biological gene functions through bioinformatic analysis. Analysis of weighted gene co-expression network analysis (WGCNA) is a systematic bioinformatic analysis which is used to recognize modules of co-expressed genes which are greatly associated with clinical practice. WGCNA promotes screening methods of complex-based differential genes that can recognize potential biological markers and therapeutic targets (6).

In the present study, WGCNA and examination of differential expression of genes were conducted on whole transcriptome of LSCC sequencing data from The Cancer Genome Atlas (TCGA) and Gene Expression Omnibus (GEO) datasets, and co-expressed differential genes and key modules were obtained. Through Gene Ontology (GO) and enrichment analyses of Kyoto Encyclopedia of Genes and Genomes (KEGG), examination of protein-protein interaction (PPI), survival analysis, protein expression validation, we further explored the molecular mechanism of the incidence and growth of LSCC.

Highlight box

Key findings

- We recognized the hub genes and key modules nearly associated to laryngeal squamous cell carcinoma (LSCC) and these genes were validated by survival analysis and the database of Human Protein Atlas.

What is known and what is new?

- LSCC is a common cancer of the head and neck, which greatly affects patients' quality of life. The pathogenesis of LSCC remains unclear.
- We identified hub genes and key modules that are closely associated with LSCC incidence and growth, and verified these genes by survival analysis and protein expression.

What is the implication, and what should change now?

- The discovery of hub genes and key modules related to LSCC is of great significance for revealing the pathogenesis of LSCC and exploring new precise biomarkers and potential therapeutic targets.

Methods

Collation of data from TCGA and GEO database

Data of gene expression in LSCC were copied from TCGA database (7) (https://portal.gdc.cancer.gov) and GEO databases (8) (https://www.ncbi.nlm.nih.gov/gds). All expression matrices and correlated clinical data of LSCC were copied through the R package *TCGAbioLinks* (9) in TCGA database. Overall, 123 samples were collected, including 111 cases of LSCC and 12 cases of normal tissue (see *Table 1*). In the GEO database, the large-sample HTS database GSE127165 was obtained using the R package *GEOquery* (10) and included 57 LSCC tissue samples and 57 adjacent normal mucosal tissue samples (see *Table 2*) (11). The study was conducted in accordance with the Declaration of Helsinki (as revised in 2013).

Screening of differentially expressed genes (DEGs)

RStudio statistical software (12) (version 1.3.959; https://rstudio.com/) and Bioconductor packages (13) (http://www.bioconductor.org/) were employed in the bioinformatic analysis of LSCC and normal tissue samples. First, raw data from the TCGA database and GEO dataset GSE127165 were gathered and brought up in accordance to the RStudio input file format software. Heatmaps and volcano plots of DEGs were drawn by the R packages *limma*, *edgeR*, *ggplot2*, and *pheatmap* (14-17). The adjusted (adj.) P values <0.05 and |logfold change (logFC)| >1 were determined statistically

Table 1 Basic characteristics of 111 LSCC samples in dataset TCGA

Parameters	Number of cases (%)
Age (years)	
≤60	47 (42.3)
>60	64 (57.7)
Gender	
Female	20 (18.0)
Male	91 (82.0)
T staging	
T1	7 (6.3)
T2	12 (10.8)
T3	25 (22.5)
T4	54 (48.6)
Unknown	13 (11.7)
Metastasis of cervical lymph node	
N0	39 (35.1)
N1	12 (10.8)
N2	39 (35.1)
N3	2 (1.8)
Unknown	19 (17.1)
Distant metastasis	
M0	40 (36.0)
M1	1 (0.9)
Unknown	70 (63.1)
Clinical stage	
I	2 (1.8)
II	9 (8.1)
III	14 (12.6)
IV	71 (64.0)
Unknown	15 (13.5)

LSCC, laryngeal squamous cell carcinoma; TCGA, The Cancer Genome Atlas.

Table 2 Basic characteristics of 57 LSCC samples in dataset GSE127165

Parameters	Number of cases (%)
Age (years)	
≤60	31 (54.4)
>60	26 (45.6)
Gender	
Female	4 (7.0)
Male	53 (93.0)
Primary site	
Glottic	30 (52.6)
Supraglottic	21 (36.8)
Subglottic	2 (3.5)
Transglottic	4 (7.0)
Differentiation	
High	8 (14.0)
Medium	37 (64.9)
Low	12 (21.1)
T staging	
T1	21 (36.8)
T2	13 (22.8)
T3	17 (29.8)
T4	6 (10.5)
Metastasis of cervical lymph node	
N0	43 (75.4)
N+	14 (24.6)
Distant metastasis	
M0	57 (100.0)
M1	0 (0.0)
Clinical stage	
I	20 (35.1)
II	10 (17.5)
III	15 (26.3)
IV	12 (21.1)

LSCC, laryngeal squamous cell carcinoma.

significant.

WGCNA

WGCNA is a systematic bioinformatic method. It is a network-based gene screening method that explores the complex relationships between highly correlated gene modules and disease phenotypes in different samples (18,19). R package *WGCNA* (6) in RStudio were used to carry out WGCNA for the LSCC gene expression data in TCGA and GEO databases. First, the sorted raw data were input, sample information and clinical data were read, and the LSCC tissue samples and normal samples were gathered. To construct the biological hub network, we fixed the optimal power value using function *PickSoftThreshold* to calculate the gene co-expression fitting index and average connectivity (20). The corresponding relationship was then transfigured to a topological overlap matrix (TOM), that was employed for sorted gathering of genes and modules of rigidity was recognized, and identical modules were gathered and merged (21). Then, the listing of genes of every single module, tree diagram of gene-module, and module-trait relationship diagram were output (22).

Overlapping of DEG analysis and WGCNA

We used R package *VennDiagram* (23) and intersected DEGs and WGCNA results to get the associated genes of LSCC. First, the modules with the most significant positive and negative associations with LSCC samples in module-trait relationship diagrams were obtained, intersected the module genes with positive and negative correlations with DEGs, and then drew two Venn diagrams. Finally, the hub intersection genes in the two Venn diagrams (24) were combined to obtain the final genes related to LSCC.

Functional and pathway enrichment analysis

The R packages *org.hs.eg. db*, *clusterProfiler*, *enrichplot*, and *ggplot2* (16,25) were used for conducting GO analysis of genes associated to LSCC, consisting of cell components (CCs), biological processes (BPs), and molecular functions (MFs) (26). These genes were analyzed by the KEGG (27) to probe the biological functions and key pathways nearly correlated with the occurrence and development of LSCC (28). Statistical significance was fix at $P<0.05$.

PPI network establishment and hub genes probing

The PPI network can provide interaction information for various proteins and help identify key genes and important modules implicated in the growth of LSCC (29). The Search Tool for the Retrieval of Interacting Genes (STRING) database (http://www.string-db.org/) was employed for establishing PPI network of candidate genes (30). Genes with minimum required interaction score ≥ 0.500 were selected to construct a whole network model that was further anticipated in Cytoscape software (http://www.cytoscape.org). Using plugin Cytohubba, the leading 10 genes with maximal clique centrality (MCC) from the candidate genes as network hub genes were chosen and visualized them (31).

Hub genes prognostic value

To validate the hub genes credibility, the interrelationship among overall survival (OS) and hub genes was tested by survival analysis of Kaplan-Meier. Using R package *survival* and *survminer* depending on TCGA database clinical data (32). We employed the online tool Gene Expression Profiling Interactive Analysis 2 (GEPIA2; http://gepia2.cancer-pku.cn/) to identify association between disease-free survival (DFS) and hub genes in LSCC patients (33). In this research work, complete follow-up information of patients was checked for analyze further, split as two divisions according to the hub genes median expression. Cut-off criteria genes of $P<0.05$ were regarded to be hub genes related to survival prognosis.

Protein expressions validation of prognostic-associated hub genes

In addition, immunohistochemistry (IHC) of the Human Protein Atlas (HPA) (https://www.proteinatlas.org/) database was employed to recognize the protein expression levels of genes associated with survivance among LSCC tissues and normal tissue samples (34). The HPA is a noteworthy dataset that gives researchers with transcriptome and proteomic information on a large number of diseased and normal tissue samples (35).

Statistical analysis

All statistical analyses were performed with RStudio

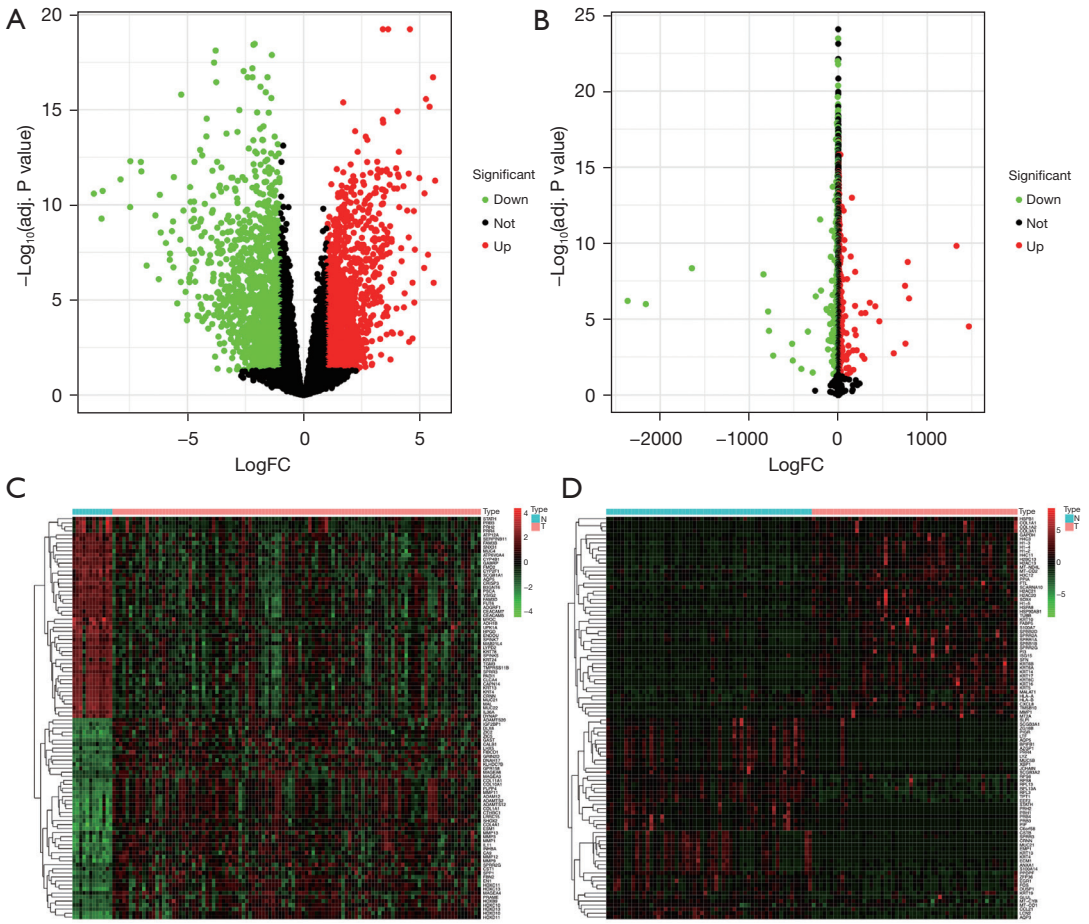

Figure 1 DEGs identification among TCGA and GEO databases of LSCC with the cut-off criteria of |logFC| ≥1.0 and adj. P<0.05. Volcano graphs of DEGs in the TCGA (A) and GEO (B) databases. Heat maps of the top 50 DEGs in the TCGA (C) and GEO (D) databases. Upregulated DEGs (red), downregulated DEGs (green). Adj., adjusted; DEG, differentially expressed gene; TCGA, The Cancer Genome Atlas; GEO, Gene Expression Omnibus; LSCC, laryngeal squamous cell carcinoma; FC, fold change.

software (2021.09.2 Build 382) and Perl (v5.30.3). Differences were statistically significant at P<0.05.

Results

DEGs identification

From the TCGA dataset, LSCC gene expression and clinical data were copied. In total, 123 samples were collected, including 111 cases of LSCC and 12 cases of normal tissue. The HTS dataset GSE127165 was copied from the GEO dataset and 57 LSCC tissue samples and 57 corresponding normal tissue samples were included. Next to data preprocessing and analysis of differential gene expression, 2,774 DEGs were obtained from TCGA database, including 1,404 upregulated DEGs and 1,370 downregulated DEGs (*Figure 1A*), and 2,139 DEGs, including 1,095 upregulated DEGs and 1,044 downregulated DEGs, were obtained from the GSE127165 dataset (*Figure 1B*). The top 50 DEGs with the most significant upregulation and downregulation are displayed by heat maps of genes (*Figure 1C,1D*). Adj. P values <0.05 and |logFC| ≥1 were used as the cut-off criteria.

WGCNA of whole transcriptome gene expression matrix

To identify identical expression trend of genes and analogy of biological functions, weighted gene co-expression network was constructed based on the RNA-sequencing (RNA-seq) count data of 14,556 genes in TCGA-LSCC

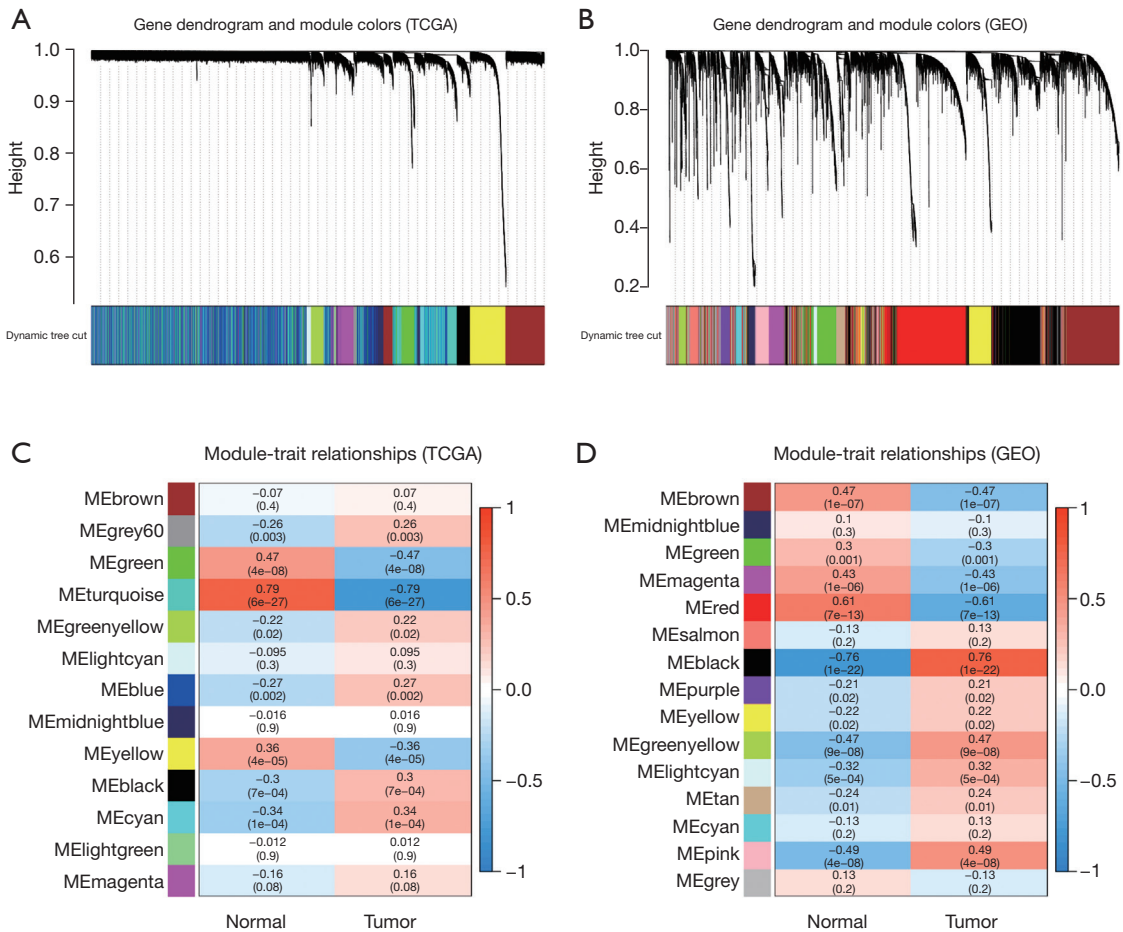

Figure 2 Recognition of modules correlated to clinical phenotype among TCGA and GEO databases of LSCC. Gene-module tree diagrams in the TCGA (A) and GEO (B) datasets. Every single branch indicates a gene, and each color below indicates one co-expressive module. Module-trait relationship diagrams in the TCGA (C) and GEO (D) datasets. Every single row correlate to a color module and column interrelated to a clinical trait (tumor or normal). Every single cell includes consistent correlation and P value. TCGA, The Cancer Genome Atlas; GEO, Gene Expression Omnibus; LSCC, laryngeal squamous cell carcinoma.

and 25,522 genes in the GSE127165 database. We recognized 13 modules from the TCGA-LSCC database (*Figure 2A*) and 15 modules from the GSE127165 dataset (*Figure 2B*) and module-trait diagrams were plotted to assess the relationship among every module and clinical phenotypes (tumor and normal). As shown in *Figure 2C*,*2D*, the MEturquoise module in TCGA-LSCC and the MEred module in GSE127165 had the greatest negative correlation with LSCC tissue, however the MEcyan module in TCGA-LSCC and the MEblack module in GSE127165 had the greatest positive correlation with LSCC tissue.

Gene recognition among WGCNA modules and the DEGs lists

According to analysis of differential expression and WGCNA, there were 2,774 DEGs in the TCGA-LSCC database and 2,139 DEGs in the GSE127165 database, 3,683 and 1,620 co-expressed genes in the MEturquoise module of TCGA-LSCC and the MEred module of GSE127165, respectively, and 249 and 1,409 co-expressed genes in the MEcyan module of TCGA-LSCC and the MEblack module of GSE127165, respectively. Overall 36

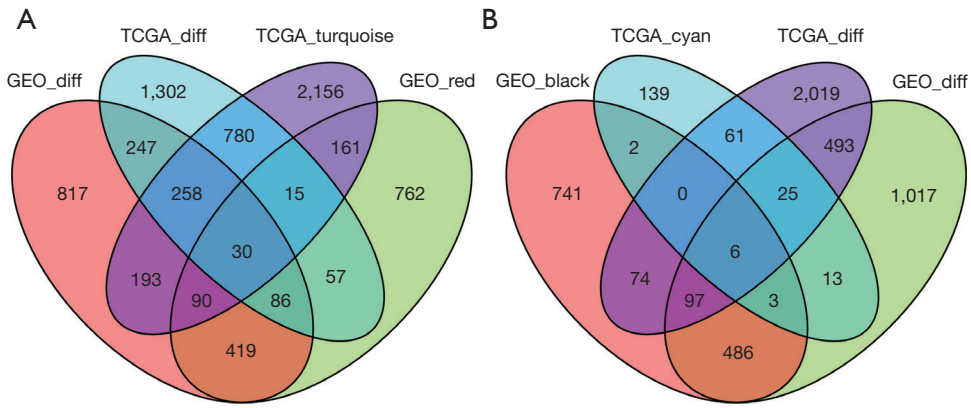

Figure 3 Venn diagrams. (A) Thirty intersecting genes among the overlapping of DEG list in two datasets [TCGA (TCGA_diff) and GEO databases (GEO_diff)] and two co-expression modules with important positive correlations [MEturquoise module of TCGA-LSCC (TCGA_turquoise) and the MEred module of GSE127165 (GEO_red)]. (B) Six intersecting genes among the overlapping of DEG list in the two datasets (TCGA_diff and GEO_diff) and two co-expression modules with the important negative correlations [MEcyan module of TCGA-LSCC (TCGA_cyan) and the MEblack module of GSE127165 (GEO_black)]. Thirty-six intersecting genes in the list of overlapping of DEG and co-expression modules. GEO, Gene Expression Omnibus; TCGA, The Cancer Genome Atlas; DEG, differentially expressed gene.

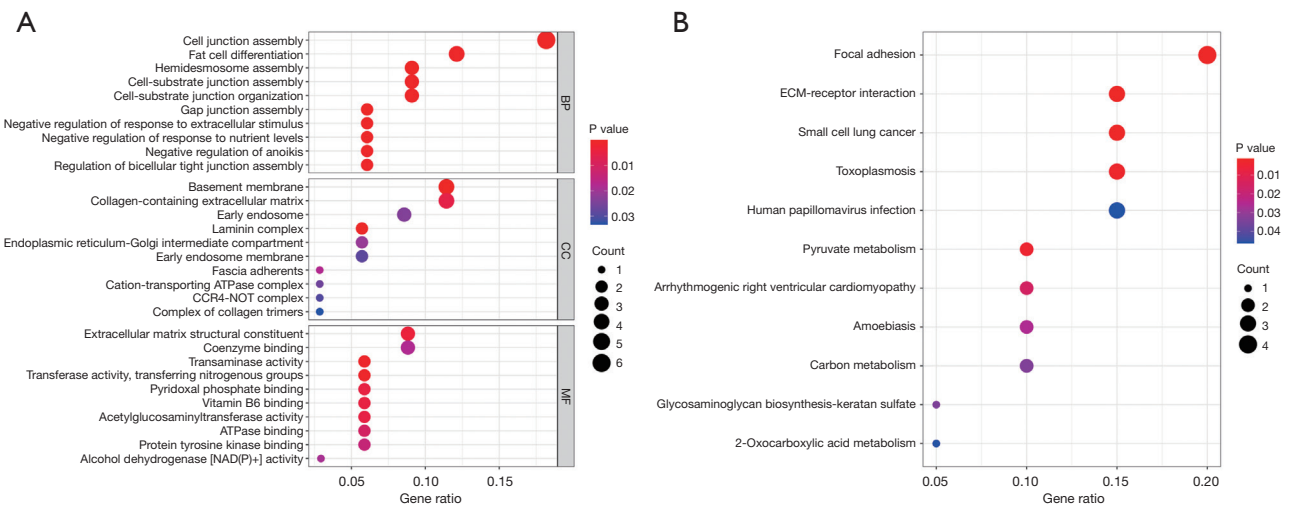

Figure 4 GO (A) and KEGG (B) enrichment examination for the 36 co-expression genes. The color indicates P values, and spots size indicates the number of genes. BP, biological process; CC, cell component; MF, molecular function; ECM, extracellular matrix; GO, Gene Ontology; KEGG, Kyoto Encyclopedia of Genes and Genomes.

intersecting co-expressed genes were retrieved for further analysis (*Figure 3A,3B*).

Thirty-six genes functional and pathway enrichment examination

GO functional and enrichment examination of KEGG pathway were conducted on the 36 intersecting co-expressed genes by the R package *cluster profiler*. GO functional enrichment analysis (*Figure 4A*) exhibited that the BP of the 36 genes were mainly concentrated in hemidesmosome assembly, cell junction assembly, and fat cell differentiation. Regarding CC, these genes were determined to be greatly associated to the basement membrane and collagen-containing extracellular matrix (ECM). In addition, in analysis of MF, ECM structural constituents and coenzyme

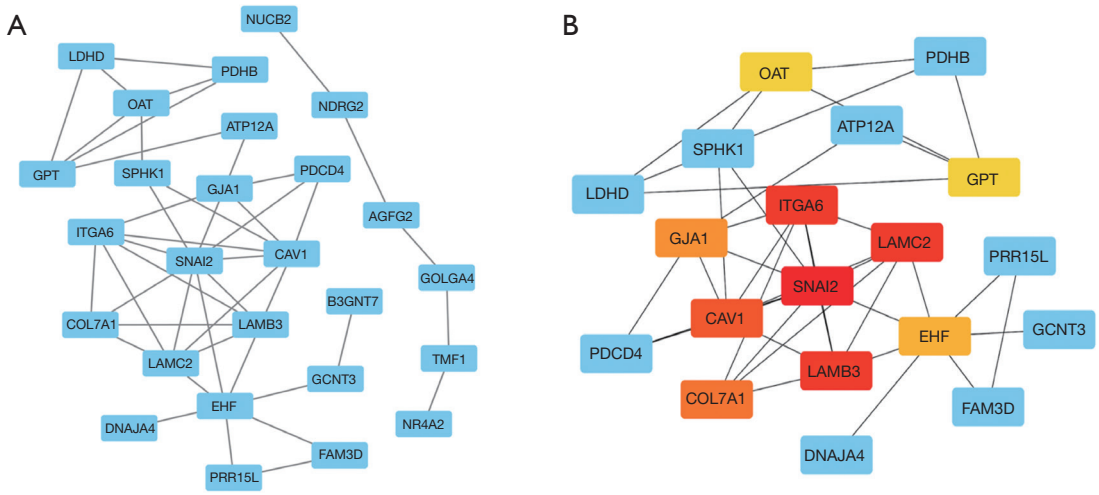

Figure 5 PPI network visualization and top 10 hub genes. (A) PPI network between the co-expression network genes. The blue node indicates the genes. The edges represent interaction associations among nodes. (B) Hub genes identification from the PPI network by MCC algorithm. The edges indicate the protein-protein associations. The red nodes indicate genes having high MCC scores, while the yellow nodes indicate genes having low MCC scores. PPI, protein-protein interaction; MCC, maximal clique centrality.

binding were considered to be associated to these 36 genes. Through enrichment examination of KEGG pathway (*Figure 4B*), we demonstrated that binding of ECM-receptor interaction, focal adhesion, small-cell lung cancer, toxoplasmosis, and HPV infection are nearly associated to these genes.

Hub genes acquisition by PPI network analysis

Using STRING database, we constructed a PPI network of the 36 overlapping co-expressed genes (*Figure 5A*). Using plug-in *Cytohubba* in the software Cytoscape, hub genes were chosen from the PPI network by the MCC algorithm are shown in *Figure 5B*. The top 10 hub genes in network are *SNAI2*, *ITGA6*, *LAMB3*, *LAMC2*, *CAV1*, *COL7A1*, *GJA1*, *EHF*, *OAT*, and *GPT*.

Survival analysis and hub genes protein expression validation

Through the above analyses, the leading 10 network hub genes (*SNAI2*, *ITGA6*, *LAMB3*, *LAMC2*, *CAV1*, *COL7A1*, *GJA1*, *EHF*, *OAT*, and *GPT*) were identified. Also by using the R package and GEPIA2 database survival analysis, OS and DFS examination of the 10 hub genes were carried out to investigate their prognosis in patients with LSCC. OS analysis showed that downregulation of *OAT* expression was remarkably associated with worse patients' prognosis with LSCC ($P<0.05$) (*Figure 6A*), while DFS analysis recommended that high expressive *CAV1* was closely related with worsening prognosis ($P<0.05$) (*Figure 6B*). Furthermore, depending on the HPA database, the *OAT* gene protein expression was remarkably reduced in tumor tissues compared with that in normal tissues (*Figure 7A*), while the *CAV1* expression was remarkably increased (*Figure 7B*).

Discussion

Laryngeal carcinoma (LC) is a malignant neoplasm that occurs in supraglottic, glottic, and subglottic regions. Squamous cell cancer (SCC) is the prominent type of cancer. At present, LSCC mainly adopts the comprehensive treatment strategy of surgical adjuvant chemoradiotherapy; however, due to the absence of accurate molecular targets, especially for patients with higher clinical stages, the prognosis is often poor. Therefore, recognizing novel

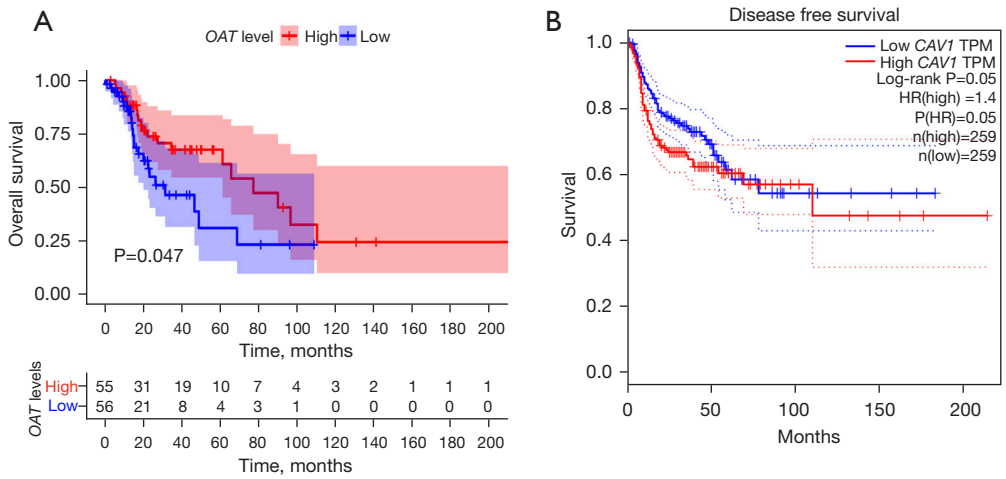

Figure 6 The leading 10 hub genes survival analysis of LSCC patients. (A) OS examination for *OAT* in LSCC by *survival* of R package. (B) Analysis of DFS for *CAV1* in LSCC from the GEPIA2 database. Stratified the patients into high-level group (red) and low-level group (green) based on the median expression of gene. P<0.05 was a statistically remarkable variation. TPM, transcript per million; HR, hazard ratio; LSCC, laryngeal squamous cell carcinoma; OS, overall survival; DFS, disease-free survival; GEPIA2, Gene Expression Profiling Interactive Analysis 2.

biological indicators and therapeutic targets is crucial for improving prognosis and LSCC patient's survival. In the present study, we employed bioinformatic analysis methods such as WGCNA to recognize 36 co-expressed DEGs in the TCGA-LSCC and GSE127165 databases. The gene functions were mainly exacerbated in cell junction assembly, basement membrane, and ECM structural constituents, and the pathways were highly concentrated in ECM-receptor interaction, focal adhesion, small cell lung cancer and toxoplasmosis. In addition, the top 10 hub genes (*SNAI2*, *ITGA6*, *LAMB3*, *LAMC2*, *CAV1*, *COL7A1*, *GJA1*, *EHF*, *OAT*, and *GPT*) were identified using the established PPI network. Low expressed *OAT* and high expressed *CAV1* remarkably influenced the LSCC patients' survival prognosis. Finally, our conclusions were confirmed by OS, DFS, and IHC analyses of *OAT* and *CAV1*.

OAT, a mitochondrial enzyme, is found highly in the liver, intestine, kidneys, and brain. An important role is to regulate the signaling molecules and mediators generation. *OAT* deficiency leads to cyclotron atrophy, an uncommon but serious genetic disorder, then illustrating the significance of this enzyme (36). Also the differential expression of *OAT* has been shown to be resulted in hepatocellular carcinoma (37), non-small cell lung cancer (38), and retinoblastoma (39). In this research work, the *OAT* expression level in LSCC tissues was significantly downregulated and nearly associated with survival prognosis. *CAV1* is an oncogenic membrane protein involved in endocytosis, metabolic alterations, cell migration, and signal transduction (40). One study found that the overexpression and secretion of *CAV1* is related to the occurrence and progression of prostate cancer (41), and is closely linked with the migration, apoptosis, proliferation and drug impedance of lung cancer cells, and can be labeled as a prognostic factor for lung cancer (42). In addition, experimental data have shown that *CAV1* can induce the expression of fucosyl transferase Pofut1 and enhance the metastasis and infiltration of mouse liver cancer cells *in vitro* and *in vivo* by activating the Notch and MAPK signaling pathways (43). The results indicate that WGCNA and other comprehensive bioinformatic analyses can reveal novel pathogenic genes and supply rich reference resources for further experimental verification.

Conclusions

In conclusion, through comprehensive bioinformatics analysis, we identified hub genes and key modules that are closely associated with LSCC incidence and growth, and verified these genes by survival analysis and protein expression. Our study is of high importance to uncover the

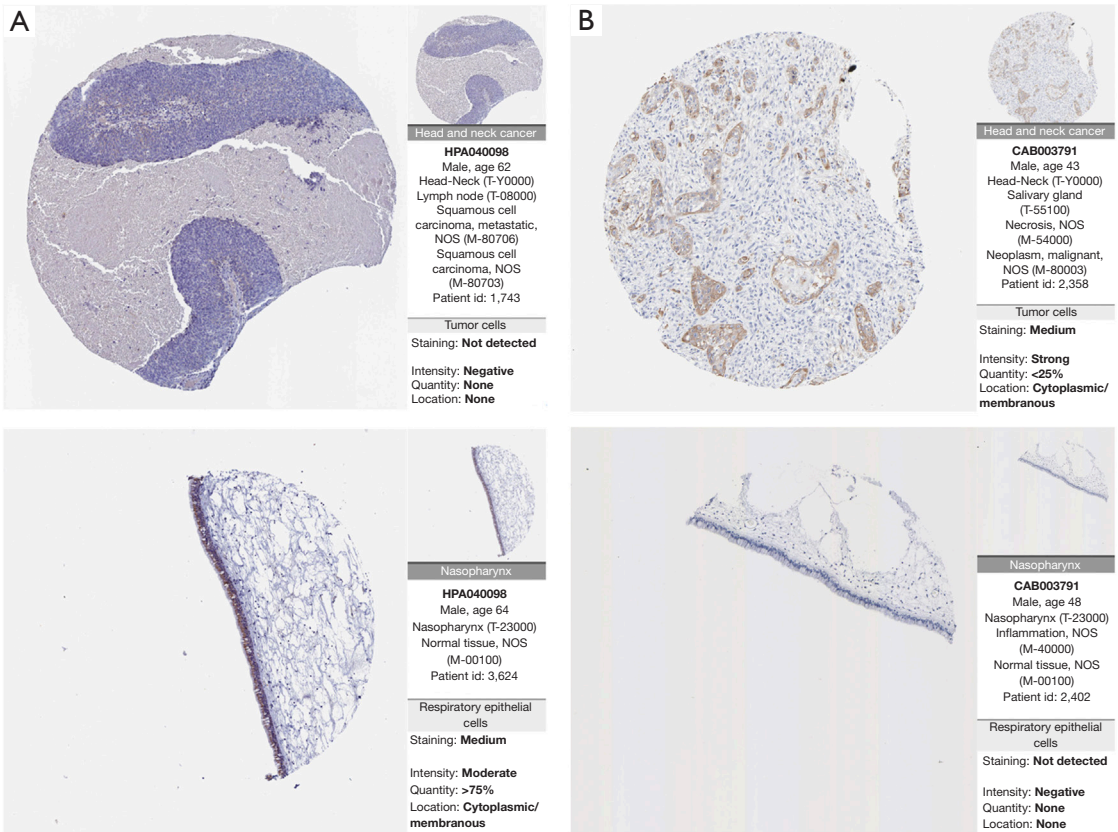

Figure 7 IHC images of the *OAT* and *CAV1* gene in tumor and normal tissues from the HPA dataset. Protein expression level of (A) OAT (https://www.proteinatlas.org/ENSG00000065154-OAT/pathology/head+and+neck+cancer#img; https://www.proteinatlas.org/ENSG00000065154-OAT/tissue/nasopharynx#img) and (B) CAV1 (https://www.proteinatlas.org/ENSG00000105974-CAV1/pathology/head+and+neck+cancer#img; https://www.proteinatlas.org/ENSG00000105974-CAV1/tissue/nasopharynx#img) in head and neck cancer and normal nasopharynx tissues). HPA, Human Protein Atlas; NOS, not otherwise specified; IHC, immunohistochemistry.

pathogenesis of LSCC and probe for new precise biological markers and potential therapeutic targets. However, studies on different subtypes and stages of LSCC are limited. Many experiments are required to further validate the genes associated with pathogenesis and prognosis of LSCC.

Acknowledgments

We thank the GEO and TCGA databases for providing all the data in this research.
Funding: None.

Footnote

Peer Review File: Available at https://tcr.amegroups.com/article/view/10.21037/tcr-24-104/prf

Conflicts of Interest: All authors have completed the ICMJE uniform disclosure form (available at https://tcr.amegroups.com/article/view/10.21037/tcr-24-104/coif). The authors have no conflicts of interest to declare.

Ethical Statement: The authors are accountable for all aspects of the work in ensuring that questions related to the accuracy or integrity of any part of the work are appropriately investigated and resolved. The study was conducted in accordance with the Declaration of Helsinki (as revised in 2013).

References

1. Machiels JP, René Leemans C, Golusinski W, et al. Squamous cell carcinoma of the oral cavity, larynx, oropharynx and hypopharynx: EHNS-ESMO-ESTRO Clinical Practice Guidelines for diagnosis, treatment and follow-up. Ann Oncol 2020;31:1462-75.
2. Riva G, Albano C, Gugliesi F, et al. HPV Meets APOBEC: New Players in Head and Neck Cancer. Int J Mol Sci 2021;22:1402.
3. Birkeland AC, Beesley L, Bellile E, et al. Predictors of survival after total laryngectomy for recurrent/persistent laryngeal squamous cell carcinoma. Head Neck 2017;39:2512-8.
4. Barrett T, Wilhite SE, Ledoux P, et al. NCBI GEO: archive for functional genomics data sets--update. Nucleic Acids Res 2013;41:D991-5.
5. Hutter C, Zenklusen JC. The Cancer Genome Atlas: Creating Lasting Value beyond Its Data. Cell 2018;173:283-5.
6. Langfelder P, Horvath S. WGCNA: an R package for weighted correlation network analysis. BMC Bioinformatics 2008;9:559.
7. Lee JS. Exploring cancer genomic data from the cancer genome atlas project. BMB Rep 2016;49:607-11.
8. Edgar R, Domrachev M, Lash AE. Gene Expression Omnibus: NCBI gene expression and hybridization array data repository. Nucleic Acids Res 2002;30:207-10.
9. Mounir M, Lucchetta M, Silva TC, et al. New functionalities in the TCGAbiolinks package for the study and integration of cancer data from GDC and GTEx. PLoS Comput Biol 2019;15:e1006701.
10. Davis S, Meltzer PS. GEOquery: a bridge between the Gene Expression Omnibus (GEO) and BioConductor. Bioinformatics 2007;23:1846-7.
11. Wu Y, Zhang Y, Zheng X, et al. Circular RNA circCORO1C promotes laryngeal squamous cell carcinoma progression by modulating the let-7c-5p/PBX3 axis. Mol Cancer 2020;19:99.
12. Aiello EN, Depaoli EG. Norms and standardizations in neuropsychology via equivalent scores: software solutions and practical guides. Neurol Sci 2022;43:961-6.
13. Silva TC, Colaprico A, Olsen C, et al. TCGA Workflow: Analyze cancer genomics and epigenomics data using Bioconductor packages. F1000Res 2016;5:1542.
14. Ritchie ME, Phipson B, Wu D, et al. limma powers differential expression analyses for RNA-sequencing and microarray studies. Nucleic Acids Res 2015;43:e47.
15. Robinson MD, McCarthy DJ, Smyth GK. edgeR: a Bioconductor package for differential expression analysis of digital gene expression data. Bioinformatics 2010;26:139-40.
16. Walter W, Sánchez-Cabo F, Ricote M. GOplot: an R package for visually combining expression data with functional analysis. Bioinformatics 2015;31:2912-4.
17. Pan Y, Wu L, He S, et al. Identification of hub genes in thyroid carcinoma to predict prognosis by integrated bioinformatics analysis. Bioengineered 2021;12:2928-40.
18. Pei G, Chen L, Zhang W. WGCNA Application to Proteomic and Metabolomic Data Analysis. Methods Enzymol 2017;585:135-58.
19. Guo H, Wang S, Ju M, et al. Identification of Stemness-Related Genes for Cervical Squamous Cell Carcinoma and Endocervical Adenocarcinoma by Integrated Bioinformatics Analysis. Front Cell Dev Biol 2021;9:642724.
20. Li Z, Huang Y, Chen X, et al. The Effect of Inflammation on the Formation of Thyroid Nodules. Int J Endocrinol 2020;2020:9827349.
21. Zhao B, You Y, Wan Z, et al. Weighted correlation network and differential expression analyses identify candidate genes associated with BRAF gene in melanoma. BMC Med Genet 2019;20:54.
22. Xing S, Liu R, Zhao G, et al. RNA-Seq Analysis Reveals Hub Genes Involved in Chicken Intramuscular Fat and Abdominal Fat Deposition During Development. Front Genet 2020;11:1009.
23. Chen H, Boutros PC. VennDiagram: a package for the generation of highly-customizable Venn and Euler diagrams in R. BMC Bioinformatics 2011;12:35.
24. Jia A, Xu L, Wang Y. Venn diagrams in bioinformatics. Brief Bioinform 2021;22:bbab108.
25. Yu G, Wang LG, Han Y, et al. clusterProfiler: an R package for comparing biological themes among gene clusters. OMICS 2012;16:284-7.
26. Lomax J. Get ready to GO! A biologist's guide to the Gene Ontology. Brief Bioinform 2005;6:298-304.
27. Kanehisa M, Goto S. KEGG: kyoto encyclopedia of genes and genomes. Nucleic Acids Res 2000;28:27-30.
28. Zhang YH, Zeng T, Chen L, et al. Determining protein-

protein functional associations by functional rules based on gene ontology and KEGG pathway. Biochim Biophys Acta Proteins Proteom 2021;1869:140621.
29. Cheng C, Hua J, Tan J, et al. Identification of differentially expressed genes, associated functional terms pathways, and candidate diagnostic biomarkers in inflammatory bowel diseases by bioinformatics analysis. Exp Ther Med 2019;18:278-88.
30. Szklarczyk D, Franceschini A, Wyder S, et al. STRING v10: protein-protein interaction networks, integrated over the tree of life. Nucleic Acids Res 2015;43:D447-52.
31. Chin CH, Chen SH, Wu HH, et al. cytoHubba: identifying hub objects and sub-networks from complex interactome. BMC Syst Biol 2014;8 Suppl 4:S11.
32. Groeneveld CS, Chagas VS, Jones SJM, et al. RTNsurvival: an R/Bioconductor package for regulatory network survival analysis. Bioinformatics 2019;35:4488-9.
33. Tang Z, Kang B, Li C, et al. GEPIA2: an enhanced web server for large-scale expression profiling and interactive analysis. Nucleic Acids Res 2019;47:W556-60.
34. Liu FJ, Wang XB, Cao AG. Screening and functional analysis of a differential protein profile of human breast cancer. Oncol Lett 2014;7:1851-6.
35. Thul PJ, Lindskog C. The human protein atlas: A spatial map of the human proteome. Protein Sci 2018;27:233-44.
36. Ginguay A, Cynober L, Curis E, et al. Ornithine Aminotransferase, an Important Glutamate-Metabolizing Enzyme at the Crossroads of Multiple Metabolic Pathways. Biology (Basel) 2017;6:18.
37. Zhu W, Doubleday PF, Catlin DS, et al. A Remarkable Difference That One Fluorine Atom Confers on the Mechanisms of Inactivation of Human Ornithine Aminotransferase by Two Cyclohexene Analogues of γ-Aminobutyric Acid. J Am Chem Soc 2020;142:4892-903.
38. Liu Y, Wu L, Li K, et al. Ornithine aminotransferase promoted the proliferation and metastasis of non-small cell lung cancer via upregulation of miR-21. J Cell Physiol 2019;234:12828-38.
39. Inana G, Totsuka S, Redmond M, et al. Molecular cloning of human ornithine aminotransferase mRNA. Proc Natl Acad Sci U S A 1986;83:1203-7.
40. Nwosu ZC, Ebert MP, Dooley S, et al. Caveolin-1 in the regulation of cell metabolism: a cancer perspective. Mol Cancer 2016;15:71.
41. Ariotti N, Wu Y, Okano S, et al. An inverted CAV1 (caveolin 1) topology defines novel autophagy-dependent exosome secretion from prostate cancer cells. Autophagy 2021;17:2200-16.
42. Shi YB, Li J, Lai XN, et al. Multifaceted Roles of Caveolin-1 in Lung Cancer: A New Investigation Focused on Tumor Occurrence, Development and Therapy. Cancers (Basel) 2020;12:291.
43. Zhang C, Huang H, Zhang J, et al. Caveolin-1 promotes invasion and metastasis by upregulating Pofut1 expression in mouse hepatocellular carcinoma. Cell Death Dis 2019;10:477.

Cite this article as: Li H, Bo S, Guo Y, Wang T, Pan Y. Identification of hub genes and key modules in laryngeal squamous cell carcinoma. Transl Cancer Res 2024;13(7):3771-3782. doi: 10.21037/tcr-24-104

